Supplementary Information: Methane trend over the last decades driven and modified by anthropogenic emissions.

Authors: Ragnhild Bieltvedt Skeie[1]*, Øivind Hodnebrog[1] and Gunnar Myhre[1]

[1] CICERO Center for International Climate Research, Oslo, Norway

* Correspondence: r.b.skeie@cicero.oslo.no

Supplementary Table 1: Anthropogenic emission inventories and scenarios used in this study. Short name used in the text, link to the emission data and references.

Short name	Link	References
CEDS-2021	https://github.com/JGCRI/CEDS/	McDuffie, et al. [1] updated
CEDS-2017	https://github.com/JGCRI/CEDS/ (CMIP6_release)	Hoesly, et al. [2]
SSPs	https://tntcat.iiasa.ac.at/SspDb/	Gidden, et al. [3]
GAINSv4	Supplementary in Höglund-Isaksson, et al. [4], post 2015 used the baseline scenario.	Höglund-Isaksson, et al. [4]
RCPs	https://tntcat.iiasa.ac.at/RcpDb/	Lamarque, et al. [5] and van Vuuren, et al. [6]
EDGARv7	https://edgar.jrc.ec.europa.eu/dataset_ghg70	Crippa, et al. [7] and EC-JRC/PBL [8]
EDGARv5	https://edgar.jrc.ec.europa.eu/dataset_ghg50	Crippa, et al. [9]

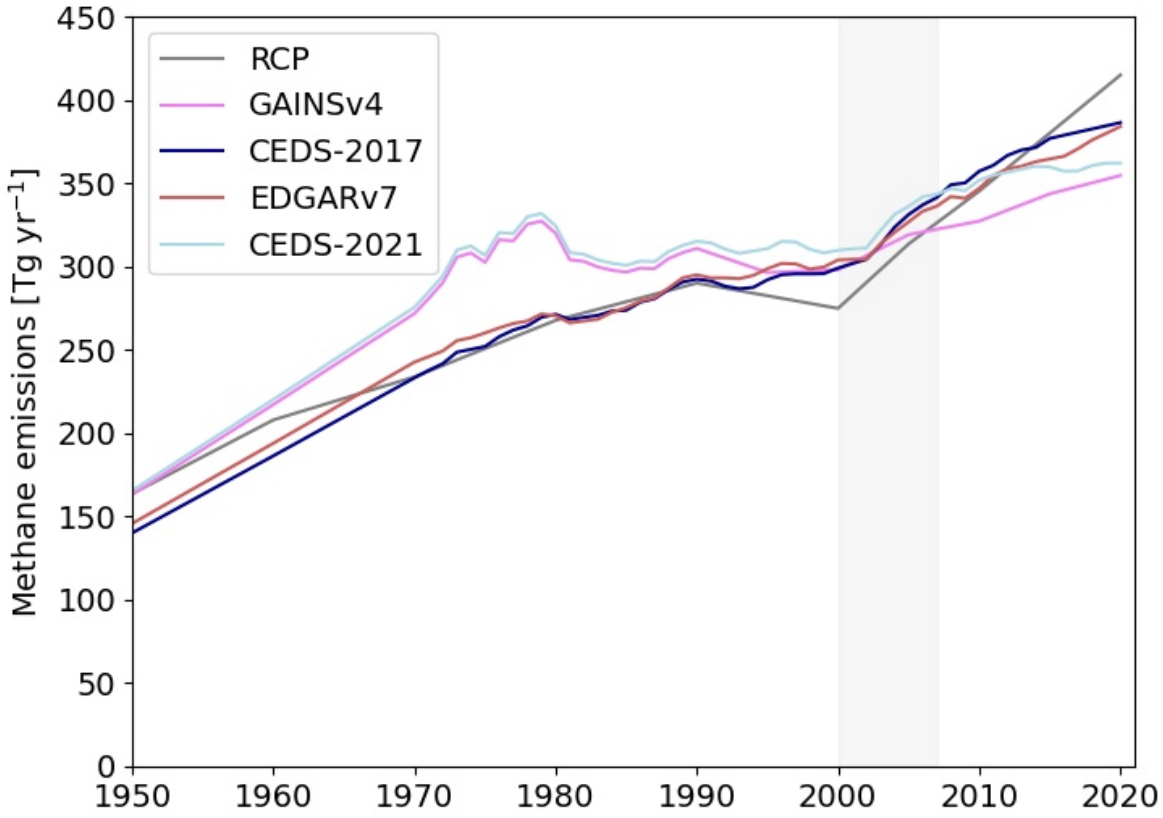

Supplementary Figure 1. The anthropogenic emissions used in the box-model. See Method section for how the emission inventories and scenarios (Table 1 and Fig. 2) are combined as all inventories do not span the entire time period.

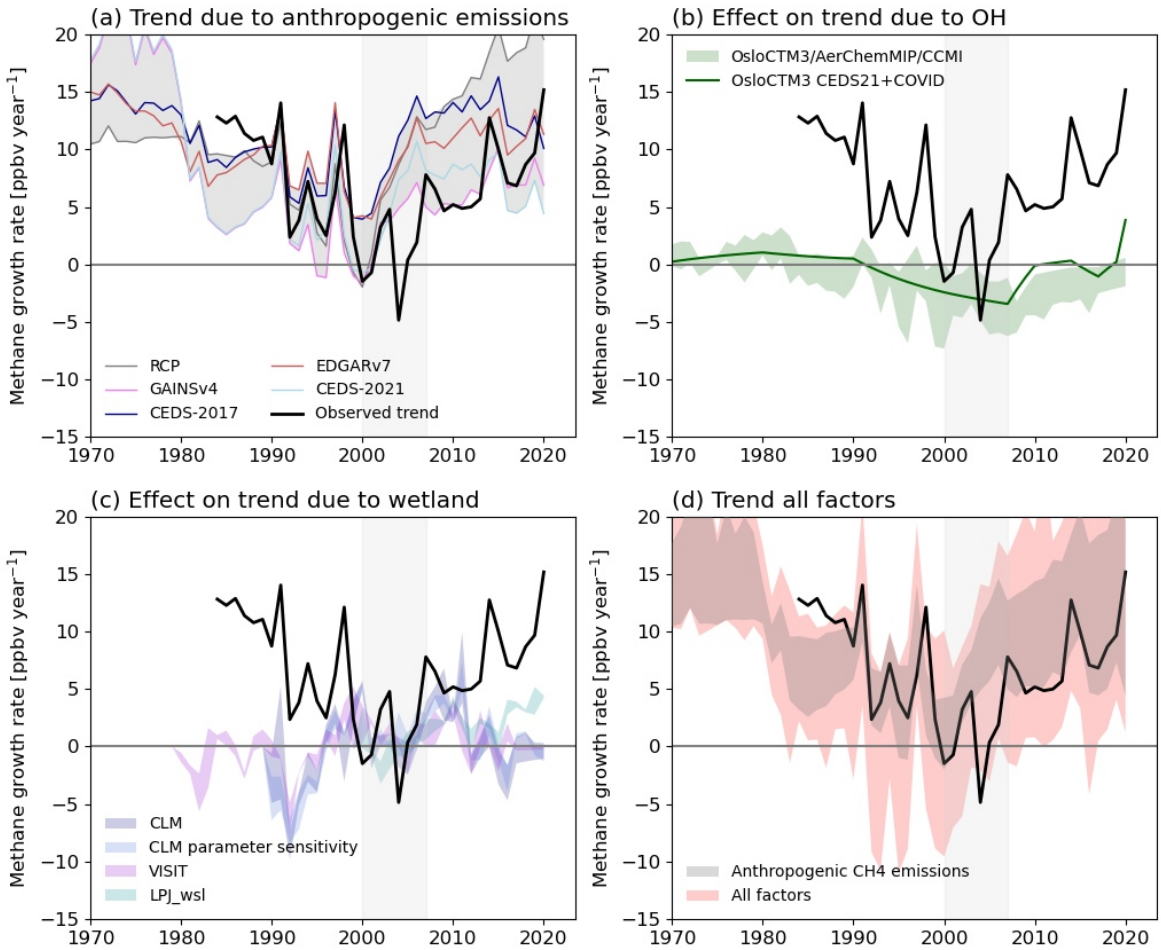

Supplementary Figure 2. Same as Fig. 1, but methane lifetime with respect to OH increased from 9.6 to 11 years in the box-model, giving a total methane lifetime of 9.5 years.

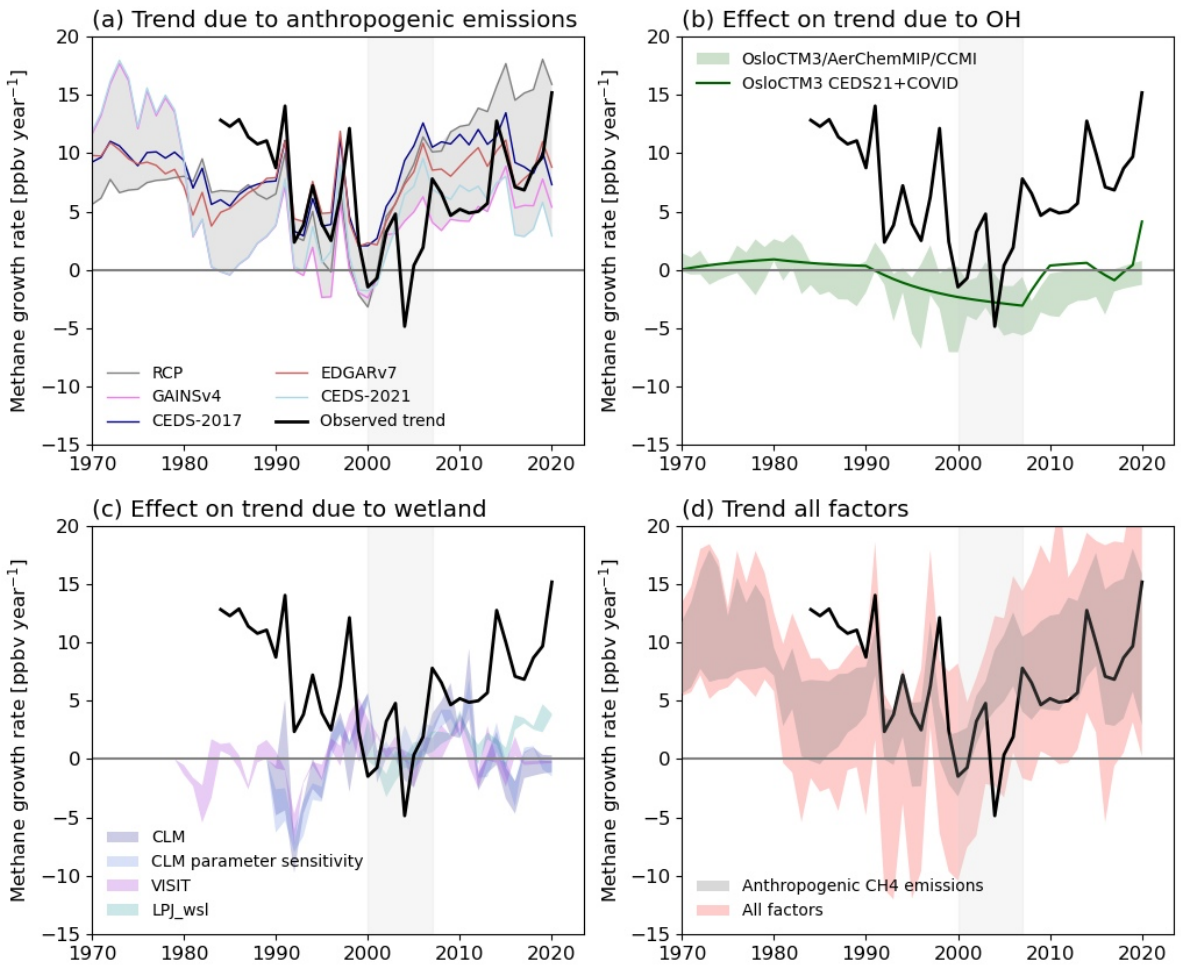

Supplementary Figure 3. Same as Fig. 1, but methane lifetime with respect to OH decreased from 9.6 to 8.2 years in the box-model, giving a total methane lifetime of 7.3 years.

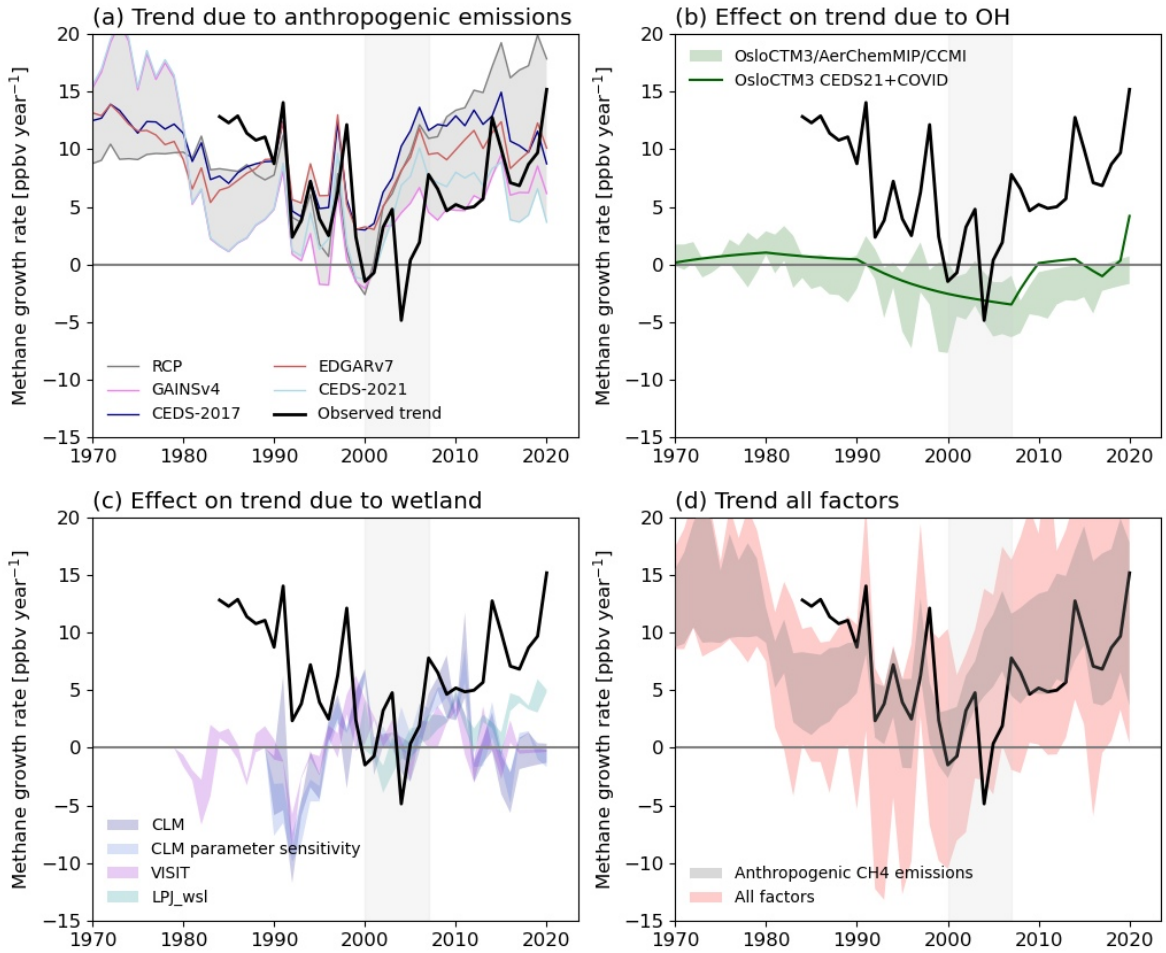

Supplementary Figure 4. Same as Fig. 1, but with enhanced wetland emissions and hence also the natural emissions in the box-model by 30 Tg yr^{-1}.

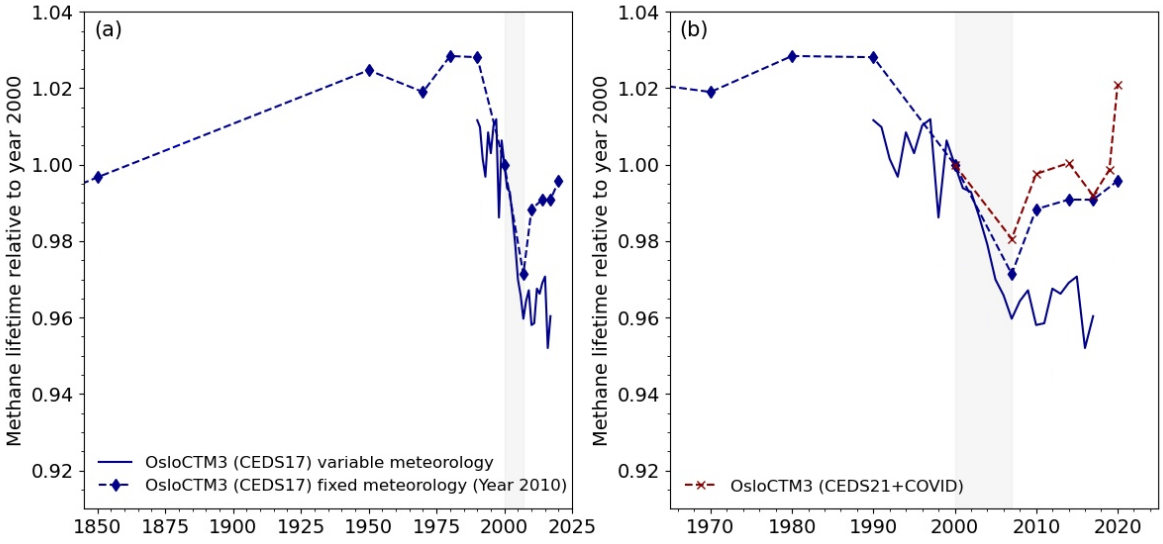

Supplementary Figure 5. Modelled methane lifetime relative to methane lifetime in year 2000. In a) results from 1850 are shown while in b) the results are shown from 1970. Results from the time-slice simulations (with the same year 2010 meteorology for all years) are shown in blue diamonds combined with dashed lines. Time development for methane lifetime changes from the simulations with variable meteorology are shown as a blue solid line. In b) the additional simulation with the CEDS-2021 emissions and COVID emission for 2020 is shown as crosses combined with dashed line. The stabilization period from 2000 to 2007 is indicated by gray shadings.

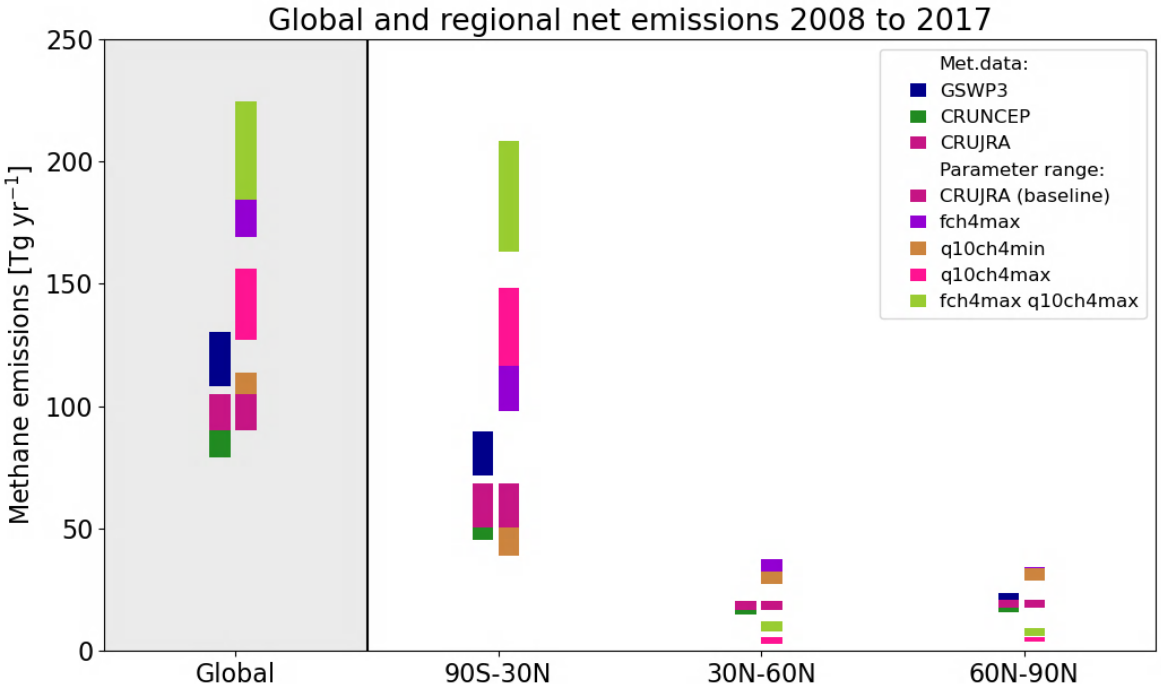

Supplementary Figure 6. Global and latitudinal net methane emissions. Coloured boxes span the annual mean values from the CLM simulations for the period 2008 to 2017 or the end year of the simulation (see Method). The CLM results are presented for two groups, simulations driven by different meteorological data (left column) and simulations driven by CRUJRA meteorological data were values for two central parameters for methane fluxes (q10ch4: q10 for methane production and f_ch4: methane production to total C mineralization rate) are varied (right column). Note that some of the coloured boxes overlap.

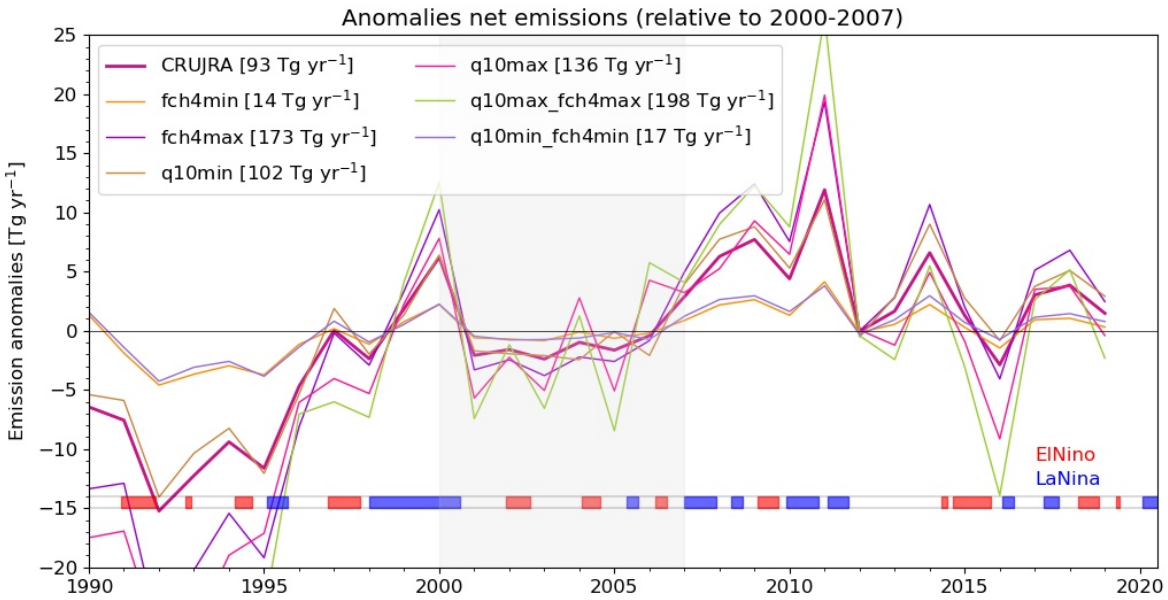

Supplementary Figure 7. Global anomalies for net methane emissions (wetland emissions, fluxes from non-inundated areas and soil sink) from 1990 to 2019 for the different sensitivity test varying two parameters (q10ch4: q10 for methane production and f_ch4: methane production to total C mineralization rate) in the biogeochemical model. The baseline simulation (CRUJRA) is shown in red and the total global emissions for the reference period (2000-2007) are indicated in the legend for each of the simulations. The ENSO phases are indicated with El Nino (red) and La Nina (blue) as in Fig. 5 and tick mark on x-axis indicate mid-year.

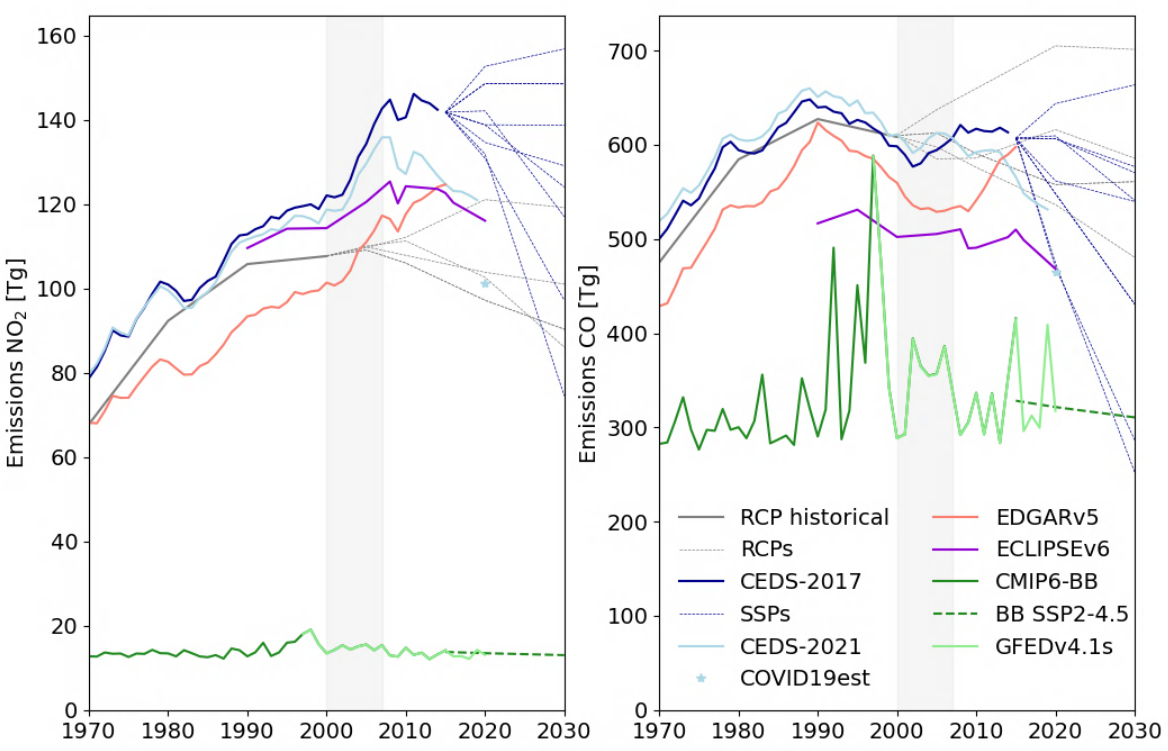

Supplementary Figure 8: Time development of total anthropogenic NOx and CO emissions for different emission inventories (Table 1) used in the NOx to CO ratio figure (Fig. 7). ECLIPSEv6 are NOx and CO emissions equivalent to GAINS methane emissions in Table 1 and the COVID19 estimate is described in the method section. Also added to the figures are biomass burning emission data plotted in green colors.

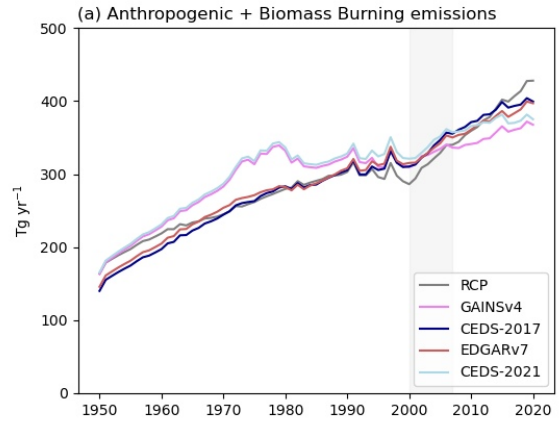

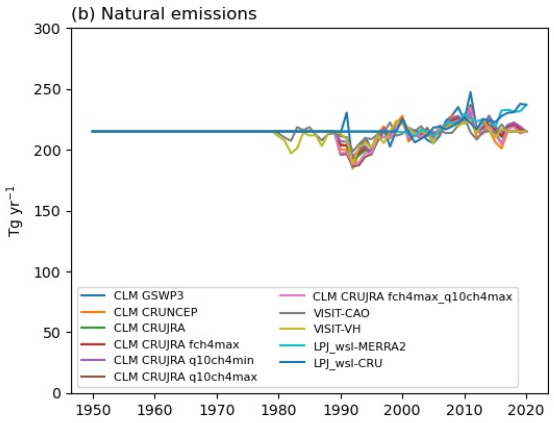

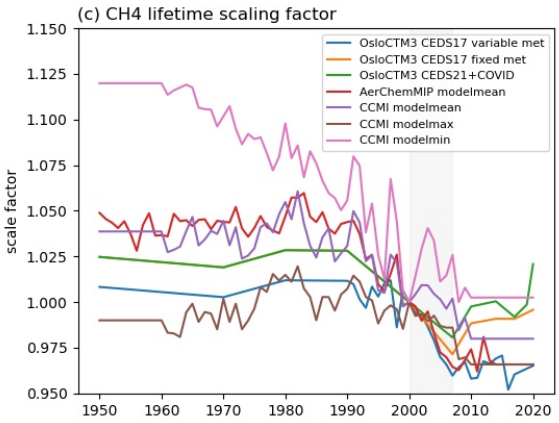

	Value
startyr	1950.0
endyear	2020.0
TAU_1	9.6
TAU_2	120.0
TAU_3	160.0
BETA_CH4	2.84
em_nat	215.0
wet_emis	149.0

Supplementary Figure 9: Input to the box-model. In a) the anthropogenic (see Fig. S1) plus biomass-burning emissions (CMIP6-BB and GFEDv4s) used, in b) the total natural emissions with emission anomalies from land modeling, in c) methane lifetime (due to OH) scaling factor used. In the table, the standard setting of the box-model is listed.

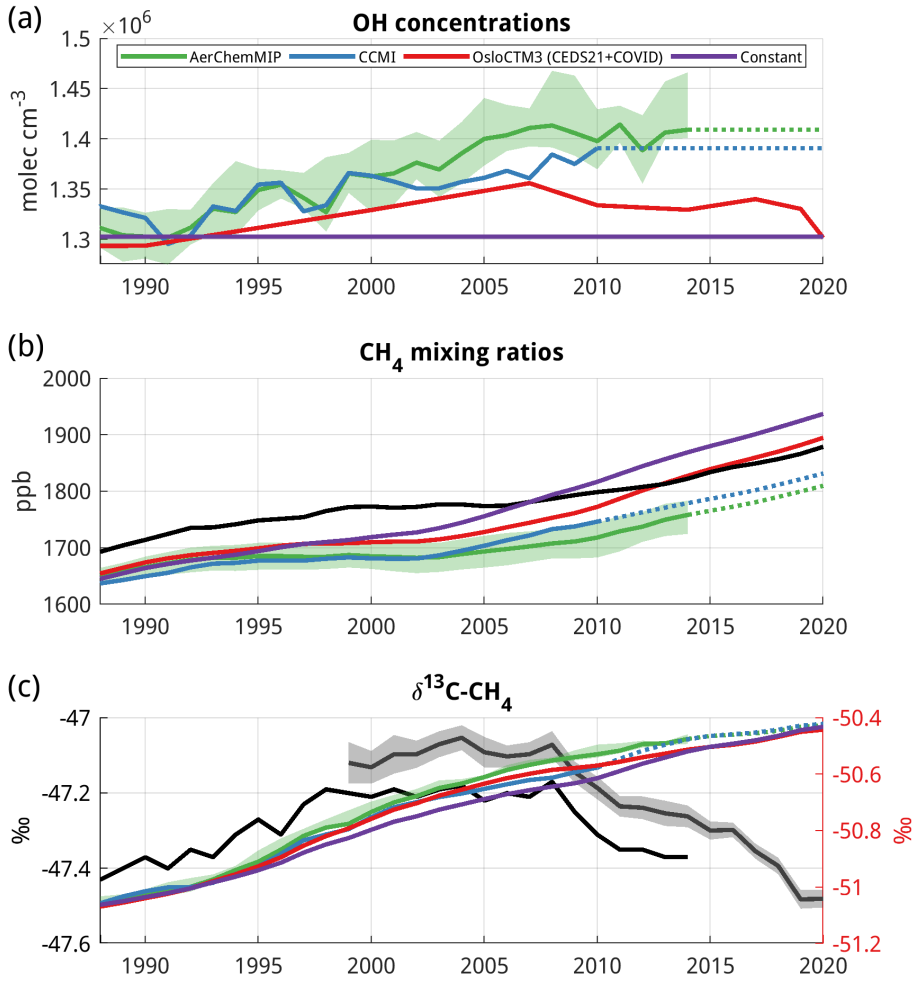

Supplementary Figure 10: a) Global OH concentration, b) CH_4 mixing ratio and c) $\delta^{13}C_{CH4}$ from isotopic box model simulations with varying OH concentration (from AerChemMIP, CCMI and OsloCTM3) and constant OH concentration (see Methods). Observed CH_4 mixing ratios are from NOAA (https://gml.noaa.gov/aggi/aggi.html), and observed $\delta^{13}C_{CH4}$ values are from Table S4 in Schaefer, et al. [10] (black line) and WMO/GAW [11] (grey line and shading) and uses the left y axis. OH concentrations from CCMI and AerChemMIP are assumed constant from 2010 and 2014, respectively (dashed lines). The green shading represents the range of OH from the different AerChemMIP models.

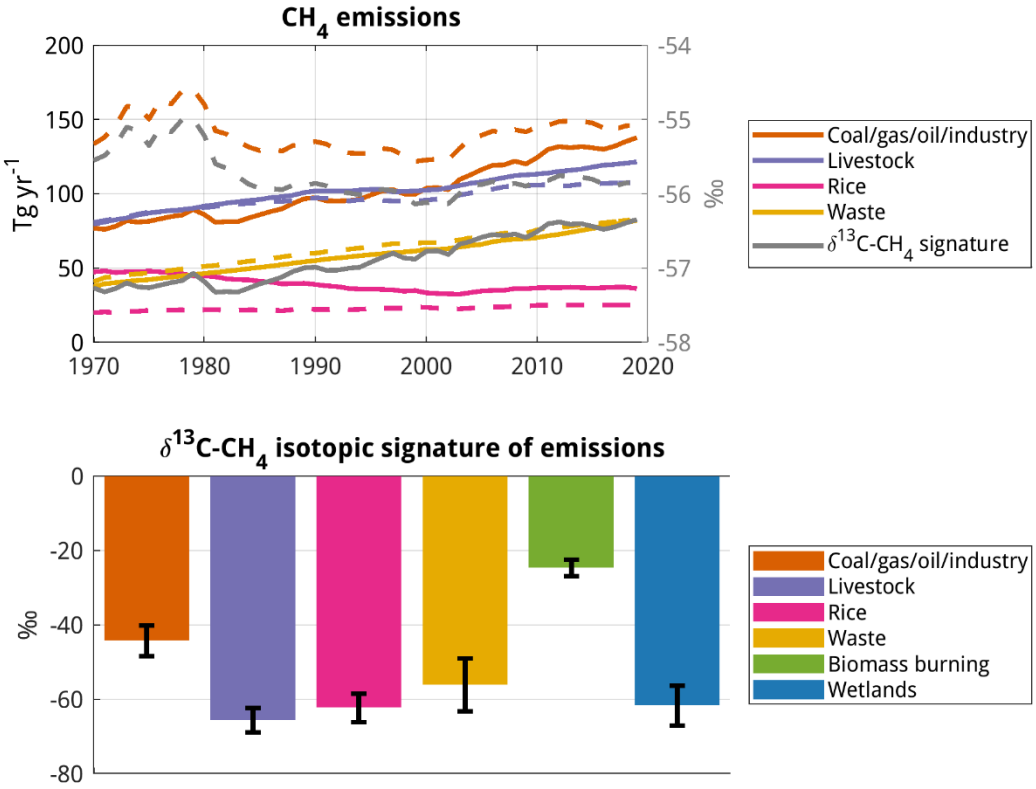

Supplementary Figure 11: Time evolution of anthropogenic emissions from EDGARv7 (solid lines) and CEDS-2021 (dashed lines) including the weighted mean of the total (based on both anthropogenic and natural emission sectors) isotopic emission signature (grey lines), and the isotopic signature for the largest emission sectors (bars and whiskers) taken from Zhang, et al. [12].

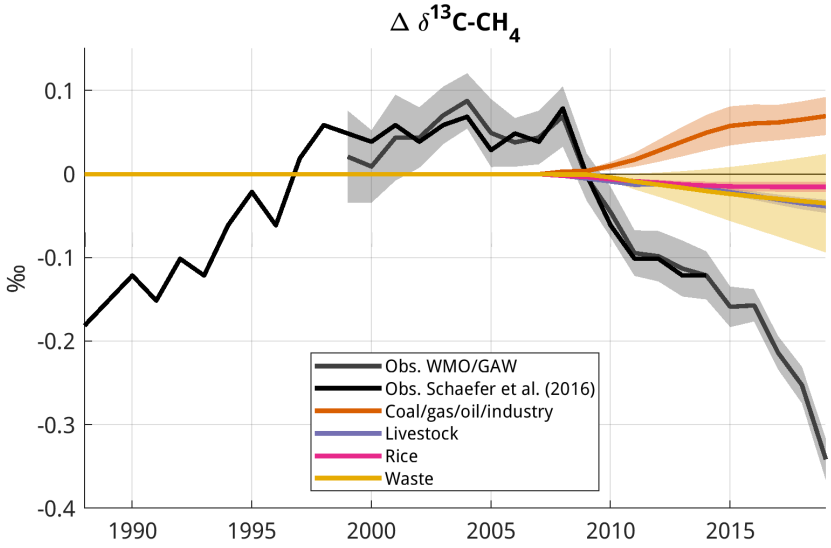

Supplementary Figure 12: Same as Figure 6b in the main manuscript, except that CEDS-2021 instead of EDGARv7 anthropogenic emissions were used in the isotopic box model.

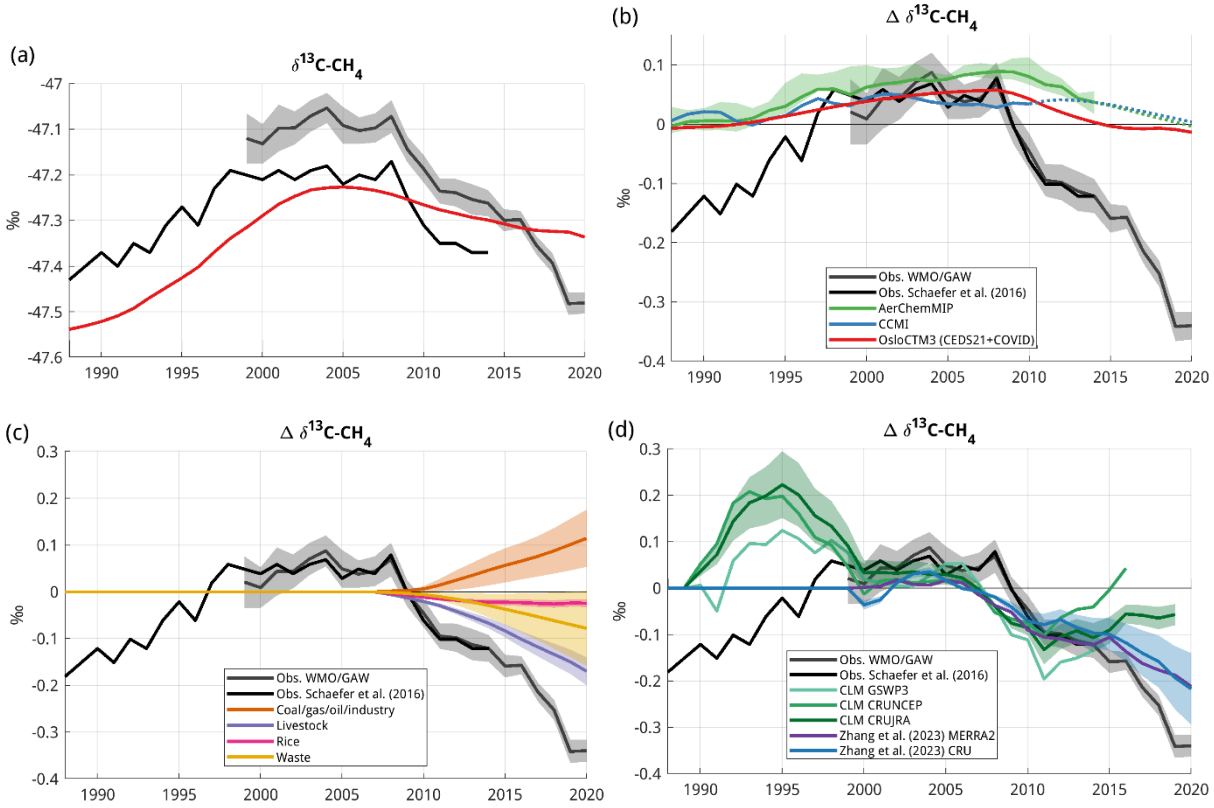

Supplementary Figure 13: a) Same as Fig. S10c and b-d) same as Figure 6a-c in the main manuscript except that the isotopic box model was tuned to better reproduce observed $\delta^{13}C_{CH4}$ values (see Methods).

Supplementary References:

1 McDuffie, E. E. *et al.* A global anthropogenic emission inventory of atmospheric pollutants from sector- and fuel-specific sources (1970–2017): an application of the Community Emissions Data System (CEDS). *Earth Syst. Sci. Data* **12**, 3413-3442, doi:10.5194/essd-12-3413-2020 (2020).

2 Hoesly, R. M. *et al.* Historical (1750–2014) anthropogenic emissions of reactive gases and aerosols from the Community Emissions Data System (CEDS). *Geosci. Model Dev.* **11**, 369-408, doi:10.5194/gmd-11-369-2018 (2018).

3 Gidden, M. J. *et al.* Global emissions pathways under different socioeconomic scenarios for use in CMIP6: a dataset of harmonized emissions trajectories through the end of the century. *Geosci. Model Dev.* **12**, 1443-1475, doi:10.5194/gmd-12-1443-2019 (2019).

4 Höglund-Isaksson, L., Gómez-Sanabria, A., Klimont, Z., Rafaj, P. & Schöpp, W. Technical potentials and costs for reducing global anthropogenic methane emissions in the 2050 timeframe –results from the GAINS model. *Environmental Research Communications* **2**, 025004, doi:10.1088/2515-7620/ab7457 (2020).

5 Lamarque, J. F. *et al.* Historical (1850–2000) gridded anthropogenic and biomass burning emissions of reactive gases and aerosols: methodology and application. *Atmos. Chem. Phys.* **10**, 7017-7039, doi:10.5194/acp-10-7017-2010 (2010).

6 van Vuuren, D. P. *et al.* The representative concentration pathways: an overview. *Clim. Change* **109**, 5, doi:10.1007/s10584-011-0148-z (2011).

7 Crippa, M. *et al.* CO2 emissions of all world countries - 2022 Report, EUR 31182 EN. (Publications Office of the European Union, Luxembourg, 2022).

8 EC-JRC/PBL. Emissions Database for Global Atmospheric Research (EDGAR), release EDGAR v7.0_FT2021_GHG (1970 - 2021) of September 2022. (2021).

9 Crippa, M. *et al.* Fossil CO2 and GHG emissions of all world countries - 2019 Report, EUR 29849 EN. (Publications Office of the European Union, Luxembourg, 2019).

10 Schaefer, H. *et al.* A 21st-century shift from fossil-fuel to biogenic methane emissions indicated by 13CH4. *Science* **352**, 80-84, doi:10.1126/science.aad2705 (2016).

11 WMO/GAW. WMO Greenhouse Gas Bulletin (GHG Bulletin) - No.18: The State of Greenhouse Gases in the Atmosphere Based on Global Observations through 2021. (2022).

12 Zhang, Z. *et al.* Anthropogenic emission is the main contributor to the rise of atmospheric methane during 1993–2017. *National Science Review* **9**, doi:10.1093/nsr/nwab200 (2022).